

Features of the Formation of Silicon Nanocrystals upon the Annealing of SiO₂ Layers Implanted with Si Ions

N. N. Ovsyuk^a, Venu Mankad^b, Sanjeev K. Gupta^b, Prafulla K. Jha^b, and G. A. Kachurin^c

^aInstitute for Geology and Mineralogy, Siberian Branch, Russian Academy of Sciences, Novosibirsk, 630090 Russia

^bDepartment of Physics, Bhavnagar University, Bhavnagar 364 002, India

^cInstitute of Semiconductor Physics, Novosibirsk, 630090 Russia

e-mail: ovsyuk@igm.nsc.ru

Abstract—The effect of annealing on the ion-beam synthesis of silicon nanocrystals in Si layers was investigated by low-frequency Raman scattering (RS). The occurrence of crystal nuclei in a matrix of glass results in an additional contribution to density of the acoustic vibrational states associated with the surface vibrational modes of nanocrystals. The low-frequency RS caused by interaction of light with acoustic vibration modes of nanoparticles is an effective method of research. The low-frequency Raman spectra show that the samples do not have a smooth distribution of nanoparticle size, but have two specific sizes of nanoparticles, 3 and 6 nm.

DOI: 10.3103/S106287381105039X

INTRODUCTION

Silicon nanocrystals have attracted much attention in recent years because of their excellent electrical and mechanical properties that are suitable for use in many areas, including biosensors [1–7]. In addition, glass doped with silicon nanocrystals can be used in optoelectronic devices. The absorption edge of these glasses can be changed by varying the composition and particle size. The optical properties of these glasses can be influenced by the quantum confinement of carriers and other dimensional effects [8–9]. Simultaneous monitoring of the size and composition of nanoparticles should further extend the scope of application of glasses doped with nanocrystals. Because the glass matrix is transparent in the visible range, the optical properties of these composite materials are determined by the nanocrystals dispersed in them. The vibrational properties of semiconductor nanoparticles are also of great interest, since phonon emission is one of the most important mechanisms of electronic dephasing. Spatial confinement of carriers changes not only the electronic structure, but also the electron-phonon interaction. Modification of phonon spectra opens a new field of nanoscale science, known as phonon engineering. This new branch of science deals with the properties of phonons and the control of the phonon dispersion in nanostructures and is called nanophononics. The creation of electronic devices with dimensions smaller than mean free path of phonons opens up new opportunities for distribution and interaction of phonons.

In recent years, techniques that could be used to modify the properties of nanostructures have begun developing. Such methods include the annealing of

SiO₂ silicon implanted glasses. If we match the annealing temperature at which nucleation occurs, but not enough for the growth of the nanoparticle size due to the diffusion flow and Ostwald ripening, it is possible to obtain nanocrystals of small size. In this work, we investigated the effect of annealing on the ion-beam synthesis of silicon nanocrystals in SiO₂ layers using low-frequency Raman spectra. Low-frequency Raman spectra associated with the interaction of visible light with acoustic vibrational modes of nanocrystals is an effective method of investigation. This is because the full density of acoustic vibrational states in the Raman spectra is observed in nanoparticles, due to the violation of the selection rules in the wave vector and in contrast to bulk crystals. It is this feature that allows us to investigate the initial stage of crystallization, since the appearance of crystalline nuclei in the glass matrix leads to an additional contribution to the density of acoustic vibrational states associated with surface vibrational modes of microcrystals. The theory of surface vibrations of a homogeneous spherical elastic body in the absence of tension at the borders was first developed by Lamb [10]. According to Lamb's theory, the frequencies of surface vibrational modes are equal to $\omega_{S0} = 0.7\omega_i/dc$ (where d is the size of a crystal nucleus, c is the velocity of light) and $\omega_{S2} = 0.85\omega_i/dc$. A detailed description of these modes is given below. It was shown previously [11] that the glass matrix also affects the natural frequencies of surface vibrations of nanocrystals, and the fractional coefficient in the above formulas depends on the polarization of light and the rigidity of the glass matrix surrounding the microcrystals. Low-frequency Raman spectra yield information on the size, shape and concentration of nuclei formed in a glass matrix.

SAMPLES AND METHODOLOGY

The samples were panes of SiO₂ glass 0.6 μm thick with implanted ions having an energy of 150 keV and a dose of 10¹⁷ cm⁻². One-time annealing for 30 minutes at 1100°C was performed. A more detailed description of the sample preparation is given in [12]. The formation of silicon nanocrystals was recorded using high-resolution electron microscopy and low-frequency Raman spectra.

THEORY

Acoustic phonons bounded in nanoparticles generate limited low-frequency modes in the vibrational spectra of these particles. These phonon modes can be attained by solving the equations of motion of a homogeneous, stress-free elastic sphere, first proposed by Lamb[10] and later developed by other authors [13, 14]. To understand the main features of the experimental Raman spectra, low-frequency vibrations of silicon nanocrystals in SiO₂ layers were calculated using three approaches: Lamb's original approach [10]; considering an isotropic sphere surrounded by a matrix [11, 14–16]; and considering a core-shell model that is applicable both to free nanoparticles and to a matrix filled with nanoparticles [17–19]. Details of Lamb's original approach can be found in [10, 20], but for the sake of comparison with the other two approaches, we shall briefly describe this model. The displacement area of elastic medium $\vec{u}(\vec{r}, t)$ with density $\rho(\vec{r})$ is governed by the Navier equation, which can be written as

$$c_{ijkl,j}\vec{u}_{k,l} + c_{ijkl}\vec{u}_{k,lj} = \rho\ddot{\vec{u}}, \quad (1)$$

where c_{ijkl} is a tensor of elastic constants of the fourth grade. The complete equation for a homogeneous isotropic medium takes the form [18]

$$(\lambda + 2\mu)\vec{\nabla}(\vec{\nabla} \times \vec{u}) - \mu\vec{\nabla} \times (\vec{\nabla} \times \vec{u}) = \rho\ddot{\vec{u}}, \quad (2)$$

where λ and μ are Lame's constants, and ρ is the density of nanoparticles. These are interconnected by the

following expressions: $V_l = \sqrt{\frac{2\mu + \lambda}{\rho}}$, and $V_t = \sqrt{\frac{\mu}{\rho}}$; V_l

and V_t are the longitudinal and transverse velocity of sound, respectively. For particles free from tension, Eq. (2) is solved by introducing scalar and vector potentials and yields two types of vibrational modes: spheroidal and torsional. These modes are described by the quantum number of orbital angular momentum l and harmonic n . The equation for the eigenvalues of the spheroidal modes takes the form [10, 20]

$$\tan\left(\frac{\omega}{V_l}a\right)/\left(\frac{\omega}{V_l}a\right) = \frac{1}{1 - \frac{1}{4}\left(\frac{\omega}{V_t}a\right)^2}, \text{ at } l = 0, \quad (3a)$$

$$\begin{aligned} & 2\left[\eta^2 + (l-1)(l+2)\left\{\frac{\eta j_{l+1}(\eta)}{j_l(\eta)} - (l+1)\right\}\right] \\ & \times \frac{\xi j_{l+1}(\xi)}{j_l(\xi)} - \frac{\eta^4}{2} + (l-1)(2l+1)\eta^2 \\ & + \left\{\eta^2 - 2l(l-1)(l+2)\right\}\frac{\eta j_{l+1}(\eta)}{j_l(\eta)} = 0, \end{aligned} \quad (3b)$$

at $l \geq 1$.

Here, η (nondimensional characteristic values) can be expressed as

$$\eta_l = \frac{\omega_l^s R}{V_t}, \quad (4)$$

where $j_l(\eta)$ and $j_l(\xi)$ are spherical Bessel functions of the first kind, and $\eta = \xi(V_l/V_t)$.

Torsional modes are transverse in nature and do not depend on a material's properties. They are determined for $l \geq 1$ and are orthogonal to the spheroidal modes [10, 20]. The spheroidal modes are characterized by moments of $l \geq 0$, where l is the symmetric breathing mode, $l = 1$ is the dipole mode, and $l = 2$ is the quadrupole mode. The mode with $l = 0$ is radial and yields polarized spectra, while the quadrupole mode with $l = 2$ yields partially depolarized spectra. Spheroidal modes for even l (i.e., with ω_{s0} and ω_{s2}) are active in RS [13]. The lowest natural frequencies for $n = 0$ and for the spheroidal and torsional modes correspond to surface modes, while modes with $n \geq 1$ are internal modes.

Lamb's simple model is able to predict only frequency (i.e., the actual position of a peak), but does not allow us to obtain the half peak observed in Raman spectra. Portalés et al. [19] therefore proposed an approach known as the core-shell model, which considers nanoparticles as a core surrounded by a macroscopically large spherical matrix that yields not only the frequencies of the modes, but also the intensity and shape of low-frequency Raman spectra. We must use the core-shell model to compare these with experimental Raman spectra. In experiments on the RS eigenvalues of vibrational modes, it is important that we have the proper values of the frequencies for which the Raman spectra intensity is associated with the mean square shift $\langle u^2 \rangle_p$ for the particle [14, 18]. In addition to the mean square shift, which determines the amplitude and shape of the spectral lines, we need to know also the matrix element of electron-phonon interaction, which determines the total intensity. The mean-square shift within the nanoparticle can be written as in [18]:

$$\langle u^2 \rangle_p = \frac{1}{V_p} \int_{R < R_p} |\vec{u}(\vec{R})|^2 d^3\vec{R}, \quad (5)$$

where V_p is the volume of a particle.

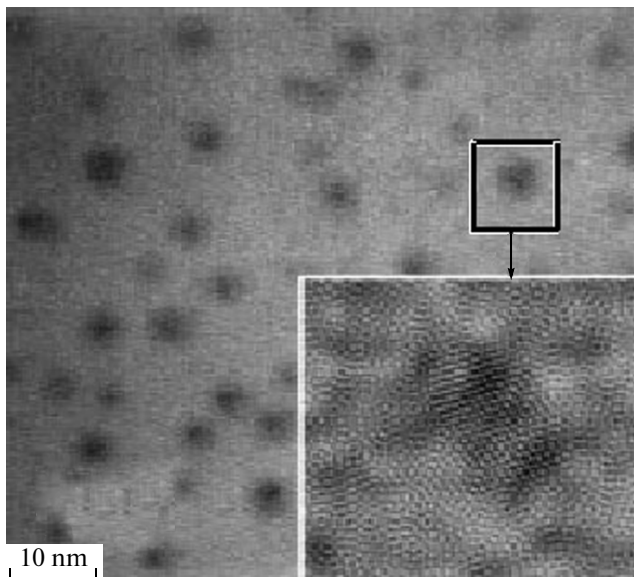


Fig. 1. High-resolution electron microscopy for cross sections of a SiO_2 glass plate with a thickness of 0.6 microns in which Si ions were implanted after annealing at 1100°C. The insert shows that the crystallinity of the inclusions is revealed after Fourier filtering at a particular site.

RESULTS AND DISCUSSION

Figure 1 shows a typical image obtained through high-resolution electron microscopy of silicon nanocrystals incorporated in SiO_2 matrix. Freely packed clusters ($\sim 6 \text{ nm}$) with differently coordinated atoms of excess silicon that have no sharp boundaries are immediately formed after the implantation of silicon. After annealing (which leads to the dominance of 4-coordinate atoms in the $\text{Si}-\text{Si}_4$ bonds), these freely packed clusters are transformed into compact precipitates ($\sim 3 \text{ nm}$), as was confirmed by high resolution electron microscopy in [21]. After implantation, there are defects that after annealing will serve as sinks for the Si atoms (i.e., nuclei for the newly formed crystals), so the Si atoms in the segregation of SiO_2 after annealing are used not for the diffusional growth of clusters, but for the formation of new nuclei. Since the minimum size of crystalline nuclei for Si is 3 nm [22], the number of nanocrystals with this size is predominant. Clusters ($\sim 6 \text{ nm}$) and nanocrystals ($\sim 3 \text{ nm}$) will thus be present in a sample, as is evidenced by the presence of two peaks in the low frequency Raman spectrum, due to the interaction of visible light with the acoustic vibrational modes of nanoparticles. These peaks were recorded using polarized scattering when the field vectors of the exciting and scattered waves were parallel to the scattering plane, i.e., they were caused by spheroidal surface modes ω_{s0} with angular moment $l=0$. For comparison with the experimental spectra, we calculated the mean square shift $\langle u^2 \rangle_p$ for Si nanoparticles of two different sizes, using the core-

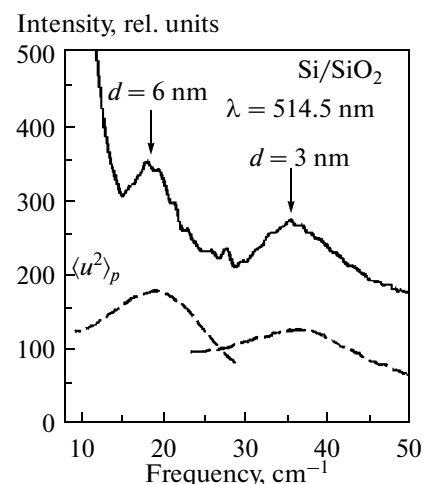


Fig. 2. Low-frequency Raman spectrum of Si nanocrystals in SiO_2 layers formed after implantation and annealing for 30 min at 1100°C. The mean-square shifts $\langle u^2 \rangle_p$ for Si nanoparticles of two sizes according to the core-shell model are shown by the dashed line.

shell model (dashed lines in Fig. 2). We used the following parameter values: $\rho_{\text{Si}} = 2.33 \text{ g/cm}^3$; $v_l = 5.95 \times 10^5 \text{ cm/s}$; $v_t = 3.76 \times 10^5 \text{ cm/s}$; $\rho_{\text{SiO}_2} = 2.2 \text{ g/cm}^3$; $v_l = 8.43 \times 10^5 \text{ cm/s}$; and $v_t = 5.84 \times 10^5 \text{ cm/s}$. It was found that the spheroidal surface modes ω_{s0} were brought down from $0.7 v_l/dc$ to $0.4 v_l/dc$ after the immersion of nanocrystals in the matrix and were equal to 38 cm^{-1} for nanocrystals with $d = 3 \text{ nm}$ and 18 cm^{-1} for clusters with $d = 6 \text{ nm}$. The calculated Raman spectrum shown in Fig. 2 turns out to be in good agreement with the experiment. The comparable half-widths of the Raman lines at 18 and 38 cm^{-1} suggest that sound is not sensitive to the smearing of the clusters' phase boundary on the atomic scale.

REFERENCES

1. Ehbrecht, M., Ferkel, H., Huisken, F., et al., *J. Appl. Phys.*, 1995, vol. 78, p. 5302.
2. Ehbrecht, M., Kohn, B., Huisken, F., et al., *Phys. Rev. B*, 1997, vol. 56, p. 6958.
3. Xia, H., He, Y.L., Wang, L.C., et al., *J. Appl. Phys.*, 1995, vol. 78, p. 6705.
4. Cheng, W., Ren Shang-Fen, *Phys. Rev. B*, 2003, vol. 65, p. 205305.
5. Seto, T., Oriii, T., et al., *Thin Solid Films*, 2003, vol. 437, p. 230.
6. Xia, Y., Yang, P., et al., *Adv. Mater.*, 2003, vol. 15, p. 353.
7. Cui, Y., Wei, Q., Park, H., and Lieber, C.M., *Science*, 2001, vol. 293, p. 1289.
8. Ekimov, A.I. and Onushchenko, A.A., *Pis'ma Zh. Eksp. Teor. Fiz.*, 1981, vol. 34, p. 363.

9. Ekimov, A.I. and Onushchenko, A.A., *Pis'ma Zh. Eksp. Teor. Fiz.*, 1984, vol. 40, p. 337.
10. Lamb, H., *Proc. London: Math. Soc.*, 1882, vol. 13, p. 189.
11. Ovsyuk, N.N. and Novikov, V.N., *Phys. Rev. B*, 1996, vol. 53, p. 3113.
12. Kachurin, G.A. Volodin, V.A., et al., *Fiz. Tekh. Poluprovodn.*, 2005, vol. 39, p. 582 [*Semiconductors* (Engl. Transl.), 2005, vol. 39, no. 5, p. 522].
13. Duval, E., *Phys. Rev. B*, 1992, vol. 46, p. 5795.
14. Talati, M. and Jha, P.K., *Phys. Rev. E*, 2006, vol. 73, p. 011901; 2008, vol. 77, p. 029904.
15. Verma, P. Cordts, W., et al., *Phys. Rev. B*, 1999, vol. 60, p. 5778.
16. Saviot, L. and Murray, D.B., *Phys. Rev. Lett.*, 2004, vol. 93, p. 055506; *Phys. Rev. B*, 2004, vol. 69, p. 094305.
17. Dubrovskii, V.A. and Morochnik, V.S., *Izv. Akad. Nauk SSSR, Fiz. Zem.*, 1981, vol. 7, p. 29.
18. Saviot, L. and Murray, D.B., *Phys. Rev. B*, 2005, vol. 72, p. 205433.
19. Portalés, H. Saviot, L., et al., *Phys. Rev. B*, 2002, vol. 65, p. 165422.
20. Saviot, L., Murray, D.B., and Marco de Lucas, M.C., *Phys. Rev. B*, 2004, vol. 69, p. 113402.
21. Kachurin, G.A. Yanovskaya, S.G., et al., *Fiz. Tekh. Poluprovodn.*, 2002, vol. 36, p. 685 [*Semiconductors* (Engl. Transl.), 2002, vol. 36, no. 6, p. 647].
22. Veprek, S., Iqbal, Z., and Sarott, F.-A., *Philos. Mag. B*, 1982, vol. 45, p. 137.